Unscented Optimal Control for Space Flight

I. Michael Ross,* Ronald J. Proulx,† and Mark Karpenko‡

Unscented optimal control is based on combining the concept of the unscented transform with standard optimal control to produce a new approach to directly manage navigational and other uncertainties in an open-loop framework. The sigma points of the unscented transform are treated as controllable particles that are all driven by the same open-loop controller. A system-of-systems dynamical model is constructed where each system is a copy of the other. Pseudospectral optimal control techniques are applied to this system-of-systems to produce a computationally viable approach for solving the large-scale optimal control problem. The problem of slewing the Hubble Space Telescope (HST) is used as a running theme to illustrate the ideas. This problem is prescient because of the possibility of failure of all of the gyros on board HST. If the gyros fail, the HST mission will be over despite its science instruments functioning flawlessly. The unscented optimal control approach demonstrates that there is a way out to perform a zero-gyro operation. This zero-gyro mode is flight implementable and can be used to perform uninterrupted science should all gyros fail.

I. Introduction

A typical space mission consists of several trajectory segments: from launch to orbit, to orbital transfers and possible reentry. The guidance and control problems for the end-to-end mission can be framed as a hybrid optimal control problem;[1] i.e., a graph-theoretic optimal control problem that involves real and categorial (integer) variables. Even when the end-to-end problem is segmented into simpler phases as a means to manage the technical and operational complexity, each phase may still involve a multi-point optimal control problem.[1] The sequence of optimal control problems is dictated by mission requirements and many other practical constraints. For instance, in its typical operation, the Hubble Space Telescope (HST) slews from one point to another point of interest. Each slew is part of a larger planning and scheduling operation that involves opportunities, priorities, science returns, capacity limits and various other constraints.[2] The gyros onboard HST provide the necessary feedback signals for slewing while the fine guidance sensors (FGS) provide the required accuracy for precision pointing.[3] Prior to 2001, normal operations required four functioning

*Professor & Program Director, Control and Optimization, Naval Postgraduate School, Monterey, CA 93943.

†Professor of Practice, Control and Optimization, Naval Postgraduate School, Monterey, CA 93943.

‡Research Assistant Professor, Control and Optimization, Naval Postgraduate School, Monterey, CA 93943. Corresponding author. E-mail: mkarpenk@nps.edu.

gyros that allowed autonomous operations of the HST in case of a single gyro failure.[4,5] In its long history, the gyros have failed and have been replaced by servicing missions. With the cancelation of these servicing missions, multiple gyro failures could doom the entire operations of the HST even though the science instruments may be working flawlessly.

Starting in 2001, the HST project began operations in a three-gyro mode.[5] While this has no effect on performance, gyro anomalies result in a temporary halt to science and hence its mission.[5] In anticipation of additional gyro failures, the HST project has developed a two-gyro science (TGS) mode.[5] In TGS mode, the rate information formerly provided by the third gyro is provided by other sensors: magnetometers, star trackers and the FGS. Because of their widely different sensor characteristics, three submodes have been defined within the TGS. Although there is no degradation in image quality in the TGS mode, there is a reduction in science productivity due to difficulty in target scheduling and constraints imposed by the star trackers.[5] A single-gyro science mode is also theoretically possible but this will have a detrimental impact on HST's science return.[6]

In this paper, we show the viability of using unscented optimal control theory to design Hubble's slews without the aid of any gyros; i.e. a true zero-gyro mode. The ideas we present in this paper are applicable to a broad range of problems beyond HST slews; for example, in [7] we apply the same concepts to solve a Zermelo problem in an uncertain environment. In principle, unscented optimal control concepts can be applied to any controllable process with uncertain parameters.

II. Introduction to Unscented Optimal Control

Julier and Uhlmann[8] introduced the unscented transform as a means to design nonlinear filters without linearization. Their concept was based on the premise that it is better to approximate a probability distribution function (PDF) than linearize a generic nonlinear function. Unscented optimal control is based on combining the unscented transform with standard optimal control to produce a new approach to directly manage navigational and other uncertainties in an open-loop framework.

Let $\mathbf{x}^0 \in \mathbb{R}^{N_x}$ be the initial random state of a nonlinear controlled dynamical system with mean, $\boldsymbol{\mu}_{x^0}$, and covariance, $\boldsymbol{\Sigma}_{x^0}$. Then, it is straightforward[8,9] to determine the sigma points, $\boldsymbol{\chi}_1^0, \boldsymbol{\chi}_2^0, \ldots, \boldsymbol{\chi}_{N_\sigma}^0$, at $t = t^0$. For simplicity of exposition, we assume a Gaussian probability distribution function (PDF) for $\mathbf{x}^0$ while noting that the concept of the unscented transform, and hence unscented optimal control, holds for non-Gaussian PDFs as well. We assume the dynamics of the nonlinear dynamical system to be given by,

$$\dot{\mathbf{x}} = \mathbf{f}(\mathbf{x}, \mathbf{u}, t) \tag{1}$$

where $\mathbf{u} \in \mathbb{U} \subseteq \mathbb{R}^{N_u}$ is the control variable, and $\mathbf{f} : (\mathbf{x}, \mathbf{u}, t) \mapsto \mathbb{R}^{N_x}$ is differentiable with respect to $\mathbf{x} \in \mathbb{X} \subseteq \mathbb{R}^{N_x}$. Then, the dynamics of each sigma point, $\boldsymbol{\chi}_i, i = 1, \ldots, N_\sigma$ is given by $\dot{\boldsymbol{\chi}}_i = \mathbf{f}(\boldsymbol{\chi}_i, \mathbf{u}, t)$. Let $\boldsymbol{X}$ be an $N_\sigma N_x$-dimensional vector given by,

$$\boldsymbol{X} := \begin{bmatrix} \boldsymbol{\chi}_1 \\ \boldsymbol{\chi}_2 \\ \vdots \\ \boldsymbol{\chi}_{N_\sigma} \end{bmatrix} \in \mathbb{R}^{N_\sigma N_x}$$

Then, the dynamics of $\boldsymbol{X}$ are given by N_σ copies of $\mathbf{f}$ given by,

$$\dot{\boldsymbol{X}} = \begin{bmatrix} \mathbf{f}(\boldsymbol{\chi}_1, \mathbf{u}, t) \\ \mathbf{f}(\boldsymbol{\chi}_2, \mathbf{u}, t) \\ \vdots \\ \mathbf{f}(\boldsymbol{\chi}_{N_\sigma}, \mathbf{u}, t) \end{bmatrix} := \mathbf{F}(\boldsymbol{X}, \mathbf{u}, t)$$

In unscented optimal control, we consider the controlled dynamical system $\dot{\boldsymbol{X}} = \mathbf{F}(\boldsymbol{X}, \mathbf{u}, t)$, whose initial state is given by the sigma points,

$$\boldsymbol{X}(t_0) = \boldsymbol{X}^0 := \begin{bmatrix} \boldsymbol{\chi}_1^0 \\ \boldsymbol{\chi}_2^0 \\ \vdots \\ \boldsymbol{\chi}_{N_\sigma}^0 \end{bmatrix}$$

The objective is to find a control trajectory, $t \mapsto \mathbf{u}$, that that drives $\boldsymbol{X}^0$ to a target state while minimizing a cost functional. Thus, the purpose of unscented optimal control is to use the concept of the unscented transform to control the statistics of the propagation.

A fundamental unscented optimal control problem can be stated in a standard format[10] as,

$$\begin{gathered} \boldsymbol{X} \in \mathbb{X}^{N_\sigma} \subseteq \mathbb{R}^{N_\sigma N_x}, \quad \mathbf{u} \in \mathbb{U} \subseteq \mathbb{R}^{N_u} \\ (U) \begin{cases} \text{Minimize} & J[\boldsymbol{X}(\cdot), \mathbf{u}(\cdot), t_f] & := E(\boldsymbol{X}(t_f), t_f) \\ \text{Subject to} & \dot{\boldsymbol{X}}(t) & = \mathbf{F}(\boldsymbol{X}(t), \mathbf{u}(t), t) \\ & (\boldsymbol{X}(t_0), t_0) & = (\boldsymbol{X}^0, t^0) \\ & \mathbf{e}(\boldsymbol{X}(t_f), t_f) & \leq \mathbf{0} \\ & \mathbf{h}(\boldsymbol{X}(t), t) & \leq \mathbf{0} \end{cases} \end{gathered} \tag{2}$$

where $E : \mathbb{X}^{N_\sigma} \times \mathbb{R} \to \mathbb{R}$ is an endpoint cost function, $\mathbf{e} : \mathbb{X}^{N_\sigma} \times \mathbb{R} \to \mathbb{R}^{N_e}$ is an endpoint constraint function that defines an endpoint set, and $\mathbf{h} : \mathbb{X}^{N_\sigma} \times \mathbb{R} \to \mathbb{R}^{N_h}$ is a path function that constrains the entire collection of sigma-point trajectories to an allowable region. The cost function, the endpoint set, and the allowable region may all be chosen by the designer to achieve various objectives.

The first major challenge in unscented optimal control theory is a problem formulation for which a solution exists. It is well-established[11,12,13] that guaranteeing the existence of a solution to a standard optimal control problem is one of the most difficult mathematical tasks. In engineering practice, the existence problem to a standard optimal control problem is not a serious hurdle to designing algorithms and producing viable solutions because the physics of the problem can be used as an intuitive guidance tool.[13,14] Because unscented optimal control is able to manage uncertainty without the use of feedback, it defies intuition; hence, significant care must be exercised in its problem formulation so that the lack of success in finding a solution from an algorithm can be attributed to the algorithm and not the existence of a solution. For these reasons, it is critical to adopt optimal control methods that offer some guarantees of a computable solution under existence hypotheses. In addition, the chosen method must be capable of handling large dimensions ($N_\sigma \times N_x$) and

producing flight implementable controllers. All of these requirements lead to the natural use of pseudospectral (PS) optimal control theory.[15] PS optimal control overcomes the curse of sensitivity by "algebraizing" the differential equations[16,17] while curbing the curse of dimensionality through spectral methods.[18,19,20] Among the large family of spectral methods, the "big two" techniques, namely, the Legendre and Chebyhsev PS methods, are the most relevant for optimal control applications.[21,22,23,24] This is because these two methods avoid the possibility of producing false positives[25,26] or divergence under mild conditions.[27] *See [15] for a comprehensive review and survey of PS optimal control theory.* Taking all these requirements into account, we follow the path of these big two PS methods that have mathematically provable convergence properties[19,28] under existence assumptions. These methods are implemented in DIDO© – the MATLAB® tool[a] for solving optimal control problems.[29] The DIDO optimal control toolbox has also a long history of flight successes in the aerospace industry.[15,30,31,32] In the rest of the sections to follow, we use DIDO for generating both the standard open-loop, as well as the unscented optimal control trajectory. In using DIDO, we also follow the pre-flight work-flow model[15] that has been used within[30,32] and outside[15,31] NASA since 2006 when PS optimal control debuted flight.[33]

III. Quantifying the Effects of Uncertainty

In its normal mode, the HST performs a standard eigenaxis slew between two points of interest using its gyros for feedback.[34] Solar-exclusion zones are managed using dog-leg maneuvers, and as will be apparent shortly, such constraints are easily handled through the use of optimal control techniques. Four reaction wheel assemblies generate the commanded control torques; see Fig. 1. Along any axis, it is possible to command a maximum torque of

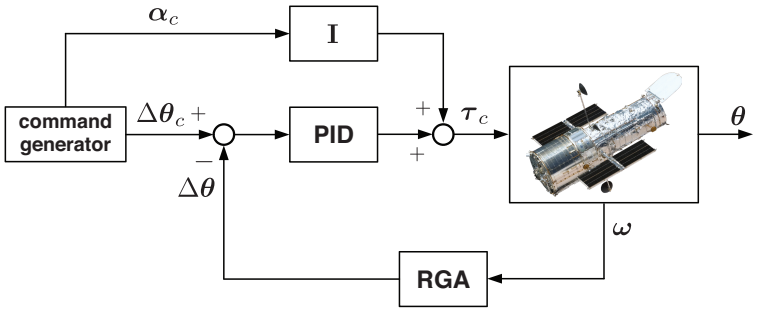

Figure 1: Block diagram of HST's pointing control system (simplified from Refs. [3] and [34]).

$0.95N.m$ with some margin left for managing uncertainties. Because this torque is generated by a momentum exchange between the reaction wheel assemblies and the main body, the maximum angular velocity of the HST is limited by 0.15 deg/s. The nominal principal moments of inertia for the HST are given by,[35] $(I_1, I_2, I_3) = (3.6, 8.7, 9.4) \times 10^4\, Kg.m^2$. At its initial time, Hubble's attitude is estimated by the FGS to an accuracy of 90 arcsec. Thus, the main unknowns for the slew are not the initial quaternions. Despite this precision in initial knowledge, in the absence of feedback from the gyros, the HST will not be able

[a] http://www.mathworks.com/products/connections/product_detail/product_61633.html

to follow the commands produced by the command generator; see Fig. 1. This is because the command generator produces signals that are not dynamically feasible[10,14] even under perfect knowledge.

In recent years, the shortest-time-maneuver[36,37,38] (STM) has emerged as a flight implementable method[b] that solves a number of these challenges through the application of optimal control techniques. Unlike the HST's command generator, the STM command is dynamically feasible and can execute an HST slew in a zero gyro mode with perfect knowledge of the initial states, inertia tensor and zero disturbance. Although the initial states are known to a very high precision, a pure STM command is not a viable option for slewing because the unknowns for the HST are the inertia tensor, the gravity gradient and the atmospheric torques. Hence, the first step in applying unscented optimal control is to quantify the effects of these unknowns. To this end, we first simulate an STM.

Let the state of the HST be represented by,

$$\mathbf{x} = \begin{bmatrix} \mathbf{q} \\ \boldsymbol{\omega} \end{bmatrix} \in \mathbb{R}^7 \tag{3}$$

where $\mathbf{q}$ and $\boldsymbol{\omega}$ are the familiar quaternions and body rates. Then, the nonlinear dynamics, $\dot{\mathbf{x}} = \mathbf{f}(\mathbf{x}, \mathbf{u})$, are given by the well-known equations,[39]

$$\begin{aligned}
\dot{q}_1 &= \frac{1}{2}\left[\omega_1 q_4 - \omega_2 q_3 + \omega_3 q_2\right] \\
\dot{q}_2 &= \frac{1}{2}\left[\omega_1 q_3 + \omega_2 q_4 - \omega_3 q_1\right] \\
\dot{q}_3 &= \frac{1}{2}\left[-\omega_1 q_2 + \omega_2 q_1 + \omega_3 q_4\right] \\
\dot{q}_4 &= \frac{1}{2}\left[-\omega_1 q_1 - \omega_2 q_2 - \omega_3 q_3\right] \\
\dot{\omega}_1 &= \frac{u_1}{I_1} - \left(\frac{I_3 - I_2}{I_1}\right)\omega_2\omega_3 \\
\dot{\omega}_2 &= \frac{u_2}{I_2} - \left(\frac{I_1 - I_3}{I_2}\right)\omega_1\omega_3 \\
\dot{\omega}_3 &= \frac{u_3}{I_3} - \left(\frac{I_1 - I_2}{I_3}\right)\omega_1\omega_2
\end{aligned} \tag{4}$$

The state and control spaces for a viable HST slew are given by,

$$\mathbb{X} := \{\mathbf{x} \in \mathbb{R}^7 : \|\mathbf{q}\|_2 = 1, \|\boldsymbol{\omega}\|_2 \leq \omega_{max}\} \tag{5}$$

$$\mathbb{U} := \{\mathbf{u} \in \mathbb{R}^3 : \|\mathbf{u}\|_2 \leq u_{max}\} \tag{6}$$

The standard STM problem is to find the state-control function pair, $t \to (\mathbf{x}, \mathbf{u}) \in \mathbb{X} \times \mathbb{U}$, that drives the spacecraft from its initial position, $\mathbf{x}(t_0) = \mathbf{x}^0$ to its target position given by $\mathbf{x}(t_f) = \mathbf{x}^f$ while minimizing the cost functional,

$$J\left[\mathbf{x}(\cdot), \mathbf{u}(\cdot), t_f\right] := t_f - t_0 \tag{7}$$

[b] http://www.nasa.gov/mission_pages/sunearth/news/trace-slew.html

For the purposes of representative analysis, we consider the boundary conditions corresponding to a large-angle-maneuver given by,

$$\begin{aligned} \mathbf{x}^0 &= [0,0,0,1,0,0,0]^T \\ \mathbf{x}^f &= [-0.27060, 0.27060, 0.65328, 0.65328, 0, 0, 0]^T \end{aligned} \tag{8}$$

These numbers corresponds to a yaw of $\psi = 90$ degrees, a pitch of $\theta = 45$ degrees and zero roll (ϕ).

For flight implementation, it is necessary to consider the impact of all of the unknowns. In pre-flight analysis, it is necessary to consider the impact of each of the unknowns separately. For this reason, we assess the impact of a $3.3\%, 1\sigma$ Gaussian uncertainty in the principal moments of inertia.

Fig. 2 shows the errors in the targeted angular position and velocity generated from 1000 Monte Carlo simulations around an STM produced by DIDO. Standard pre-flight verification

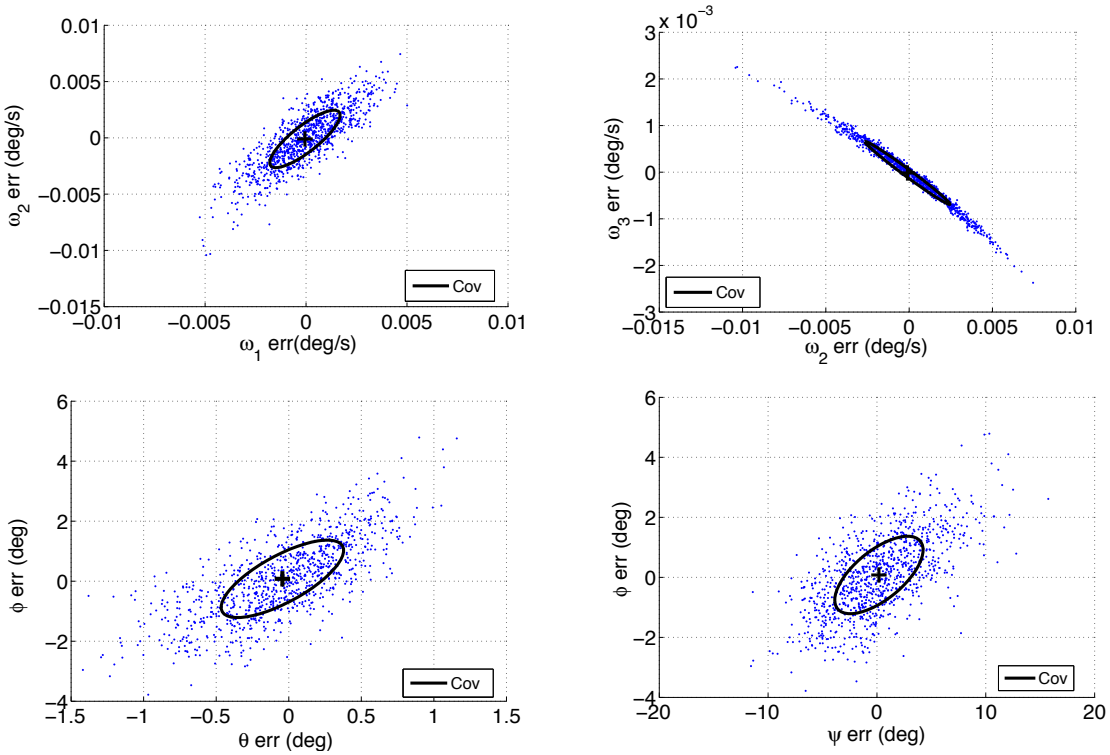

Figure 2: Monte Carlo simulations of target error distributions produced by an STM implementation for the HST in a zero-gyro mode.

and validation tests were performed on the STM; see [15,30] for additional details. From the statistics of the errors provided in Table 1, the mean angular velocity is off of its targeted value by about 0.2 arcsec/s while the mean angular position is off by a whopping 741 arcsec. Obviously, the HST will not be able to perform its mission in an open-loop zero-gyro framework. Thus, a possible first step in developing a zero-gyro framework is to explore the possibility of targeting zero mean.

Target Parameter	Error Mean	Standard Deviation
ω_1(arcsec/s)	-0.197	6.26
ω_2(arcsec/s)	-0.356	9.18
ω_3(arcsec/s)	-0.063	2.43
ψ (arcsec)	666.0	14,616
θ (arcsec)	-158.0	1519
ϕ (arcsec)	284.0	4644

Table 1: Quantification of the errors in the targeted values of angular position and velocity computed from 1000 Monte Carlo simulations

IV. Initial Unscented Problem Formulation: Targeting Zero Mean

As noted before, we assume no uncertainty in the initial states, $\mathbf{x} := (\mathbf{q}, \boldsymbol{\omega})$, as a result of the availability of the FGS; hence, the HST dynamical model is parameterized by uncertainties in the three principal moments of inertia,

$$\dot{\mathbf{x}} = \mathbf{f}(\mathbf{x}, \mathbf{u}; I_1, I_2, I_3)$$

From Julier's second order minimal simplex method,[40] we have $N_\sigma = 5$. Hence, the state space for the unscented HST optimal control problem is $\mathbb{X}^5 = \mathbb{R}^{35}$, and the state variable, $\boldsymbol{X}$, comprises five copies of $(\mathbf{q}, \boldsymbol{\omega})$. Each of these five copies of the state vector starts at the same initial point, $\boldsymbol{\chi}_j(t_0) = \mathbf{x}^0,\ j = 1, \ldots, 5$, with the same dynamical law but with five different velocities,

$$\dot{\boldsymbol{\chi}}_j = \mathbf{f}(\boldsymbol{\chi}_j, \mathbf{u}; I_1^j, I_2^j, I_3^j) \qquad j = 1, \ldots, 5$$

where $I_1^j, I_2^j, I_3^j,\ j = 1, \ldots, 5$ are the values of the principal moments of inertia that correspond to the five sigma points. Each evolution of the state trajectory, $t \mapsto \boldsymbol{\chi}_j$, must satisfy the state-space constraints,

$$\left\{\boldsymbol{\chi}_j(t) = (\mathbf{q}_j(t), \boldsymbol{\omega}_j(t)) :\ \|\mathbf{q}_j(t)\|_2 = 1, \quad \|\boldsymbol{\omega}_j(t)\|_2 \leq \omega_{max}\right\} \quad \forall\, j = 1, \ldots, 5$$

We now pose the constructive question: is it possible to drive the evolutions of the state trajectories such that the final value of the mean sigma-point vector, $\boldsymbol{\mu}_\chi(t_f)$, is equal to the target value given by $\mathbf{x}^f$? Using the unscented optimal control framework, we explore this question by stipulating that the final-time conditions satisfy the equality constraint,

$$\mathbf{e}(\boldsymbol{X}(t_f)) := \boldsymbol{\mu}_\chi(t_f) - \mathbf{x}^f = \mathbf{0}$$

Care must be taken in computing $\boldsymbol{\mu}_\chi$ in ensuring that the norm constraint $\|\mathbf{q}\|_2 = 1$ is satisfied. A minimum time unscented optimal control problem can be posed as finding the open-loop control trajectory, $t \mapsto \mathbf{u}$, that minimizes the endpoint cost functional,

$$E(\boldsymbol{X}(t_f), t_f) := t_f - t_0$$

while satisfying all the constraints. As this is now a standard optimal control problem, albeit a high-dimensional one, it can be solved. In fact, because of its high dimension, it makes

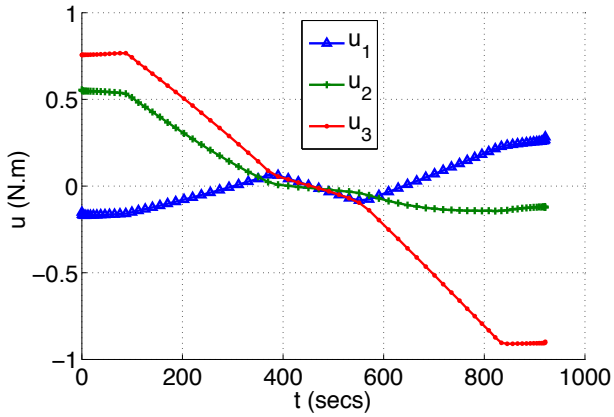

Figure 3: Unscented optimal control for targeting a zero mean error.

one of the strongest cases for the use of the big two PS methods[15] implemented in DIDO. The unscented optimal control generated by DIDO is shown in Fig. 3. The corresponding sigma point state trajectories are shown in Fig. 4.

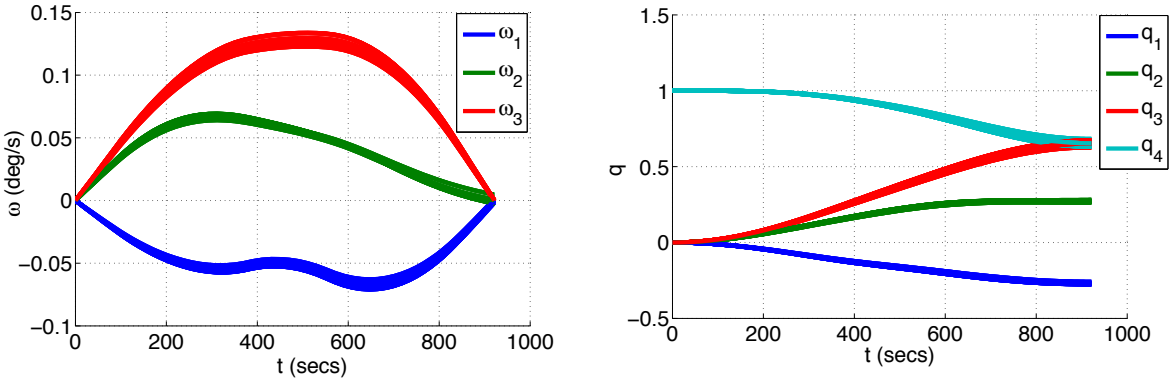

Figure 4: Sigma point state trajectories for the HST that target a zero mean error.

It is apparent from these figures that the state-space constraints (see Eqs. 5 and 6) are met by all of the sigma point trajectories. From the statistics of the endpoint values, provided in Table 2, it is clear that the mean is near zero — a far better proposition than the standard open-loop statistics of Table 1. Note, in particular, the error mean in the target angles is about 1 milli-arc seconds.

It is apparent that the unscented optimal control solution is implementable (see Fig. 3) as a zero-gyro solution for the HST; however, it can be reasonably argued that the approach may still be risky because the covariances in Table 2 are about the same order of magnitude as those of Table 1. This perspective is amplified in Fig. 5 where two illustrative covariance ellipses are plotted as a means to clarify this point: the means are within milli-arc seconds of the target but but the spread is in the neighborhood of about a degree. Hence, we now seek to determine a lower risk solution by exploring the possibility of controlling the variances at the target point.

Target Parameter	Error Mean	Standard Deviation
ω_1(arcsec/s)	-2.44 E-15	4.10
ω_2(arcsec/s)	2.10 E-14	9.47
ω_3(arcsec/s)	-2.55 E-15	1.26
ψ (arcsec)	1.20 E-07	14,112
θ (arcsec)	-2.72 E-08	1476
ϕ (arcsec)	8.89 E-08	5760

Table 2: Error statistics from an unscented optimal control that targets a zero mean.

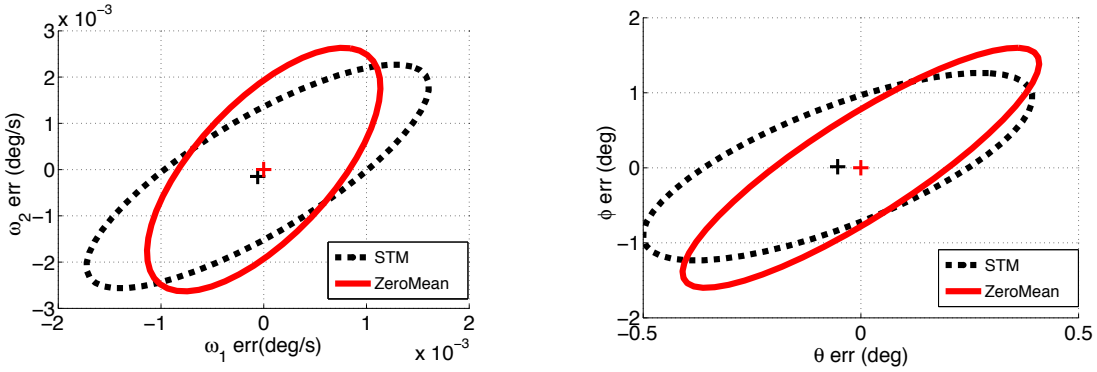

Figure 5: Two illustrative covariance ellipses for one instantiation of an unscented optimal control compared against that of a standard open-loop controller; the cross-hairs denote the relevant means.

V. Risk-Reduced Unscented Problem Formulation

We propose to reduce the risk associated in the open-loop control of the previous section by controlling the spread of the final values of the sigma points. One measure of this spread is the variance; hence, we propose an additional set of terminal conditions given by,

$$\text{diag}\big[\boldsymbol{\Sigma}_{\mathbf{y}(\chi)}(t_f)\big] \leq [\sigma_\psi^2, \sigma_\theta^2, \phi_\phi^2, \sigma_{\omega_1}^2, \sigma_{\omega_2}^2, \sigma_{\omega_3}^2]^T$$

where $\sigma_{(\cdot)}^2$ are user-specified values of the respective variances and $\mathbf{y}$ represents the transformation from the quaternion space to the space of Euler angles. Thus, the new set of endpoint conditions for this problem are given by,

$$\mathbf{e}_1(\boldsymbol{X}(t_f)) := \boldsymbol{\mu}_\chi(t_f) - \mathbf{x}^f = \mathbf{0} \tag{9}$$

$$\mathbf{e}_2(\boldsymbol{X}(t_f)) := \text{diag}\big[\boldsymbol{\Sigma}_{\mathbf{y}(\chi)}(t_f)\big] \leq [\sigma_\psi^2, \sigma_\theta^2, \phi_\phi^2, \sigma_{\omega_1}^2, \sigma_{\omega_2}^2, \sigma_{\omega_3}^2]^T \tag{10}$$

Following the same process as before, the statistics resulting from this solution are given in Table 3. Comparing the last column of Table 3 with that of Table 2, it is clear that this problem formulation has achieved a ten-fold reduction in risk. This point is further elaborated in Fig. 6 where two illustrative covariances of both instantiations of unscented optimal control techniques are plotted.

Target Parameter	Error Mean	Standard Deviation
ω_1(arcsec/s)	3.60 E-02	0.341
ω_2(arcsec/s)	-6.77 E-12	.932
ω_3(arcsec/s)	6.77 E-13	.130
ψ (arcsec)	1.24 E-06	1,436
θ (arcsec)	-1.16 E-06	153
ϕ (arcsec)	1.19 E-06	619

Table 3: Error statistics from an unscented optimal control that targets a zero mean and a given value of risk.

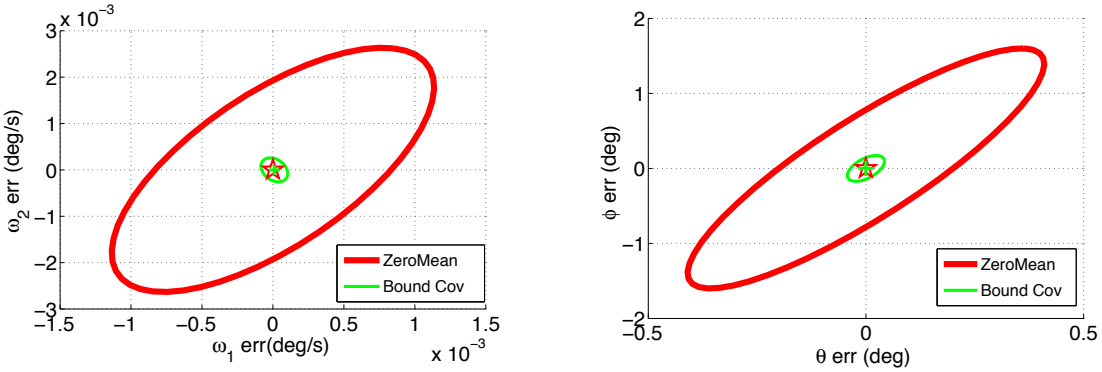

Figure 6: Demonstration of a ten-fold reduction in the covariances of the target values of sample state variables.

VI. Conclusions

Since the 2006 flight implementation of Bedrossian's zero propellant maneuver on board the International Space Station, optimal control techniques have become routine over a large segment of the aerospace industry. The routine use of these techniques has opened up new challenges in guidance and control where the objectives are higher performance at reduced costs with demands for graceful degradation in the event of failures, unforseen uncertainties and other unknowns. The traditional means to manage these uncertainties is feedback; however, in the absence of feedback there is no room for graceful degradation. Furthermore, a management of uncertainties through the use of feedback principles alone is no longer the discriminating concept for inexpensive control systems. An unscented control offers an inexpensive and simple means to manage uncertainties in the absence of feedback. In the case of the Hubble Space Telescope, given that servicing missions are no longer viable, the entire science project will come to a standstill if all of the gyros fail. The unscented optimal control solution offers a simple and viable approach to perform continued science.

References

[1]Ross, I. M. and D'Souza, C. D., "Hybrid Optimal Control Framework for Mission Planning," *Journal of Guidance, Control and Dynamics*, Vol. 28, No. 4, pp. 686-697, July-August 2005.

[2]Muscettola, N., *HSTS: Integrating Planning and Scheduling*, Carnegie Mellon University Technical Report, CMU-RI-TR-93-05, Pittsburgh, PA, March 1993.

[3]Dougherty, H., Tompetrini, K. Levinthal, J. and Nurre, G., "Space Telescope Pointing Control System," *Journal of Guidance, Control and Dynamics*, Vol. 5, No. 4, 1982, pp. 403-409.

[4]Markley, F. L. and Nelson, "Zero-Gyro Safemode Controller for the Hubble Space Telescope," *Journal of Guidance, Control and Dynamics*, Vol. 17, No. 4, 1994, pp. 815-822.

[5]Prior, M. and Dunham, L., "System Design and Performance of Two-Gyro Scince Mode for the Hubble Space Telescope," *Acta Astronautica*, Vol. 61, 2007, pp. 1010-1018.

[6]Harwood, W., "Healthy Hubble Telescope Raises Hopes of Longer Life," *Spaceflightnow.com*, Posted June 1, 2013.

[7]Ross, I. M., Proulx, R. J., and Karpenko, M., "Unscented Optimal Control for Orbital and Proximity Operations in an Uncertain Environment: A New Zermelo Problem," *AIAA Space and Astronautics Forum and Exposition: AIAA/AAS Astrodynamics Specialist Conference*, San Diego, CA 4-7 August 2014.

[8]Julier, S. J. and Uhlmann, J. K., "A New Extension of the Kalman Filter to Nonlinear Systems," *Proceedings of AeroSense: The 11th International Symposium on Aerospace/Defense Sensing, Simulation and Controls*, Orlando, FL, SPIE 1997. Multi Sensor Fusion, Tracking and Resource Management II.

[9]Julier, S. J., Uhlmann, J. K. and Durrant-Whyte, H. F. "A New Approach for Filtering Nonlinear Systems," *Proceedings of the American Control Conference*, Seattle, WA, 1995, pp. 1628-1632.

[10]Ross, I. M. *A Primer on Pontryagin's Principle in Optimal Control*, Collegiate Publishers, San Francisco, CA, 2009.

[11]Vinter, R. B., *Optimal Control*, Birkhäuser, Boston, MA, 2000.

[12]Clarke, F. H., Ledyaev, Y. S., Stern, R. J., and Wolenski, P. R., *Nonsmooth Analysis and Control Theory,* Springer-Verlag, New York, NY, 1998.

[13]Longuski, J. M., Guzmán, J, J., and Prussing, J. E., *Optimal Control with Aerospace Applications*, Springer, New York, N.Y., 2014.

[14]Ross, I. M. and Gong, Q., *Emerging Principles in Fast Trajectory Optimization, Sixth Edition*, Elissar Global, Carmel, CA, 2013.

[15]Ross, I. M. and Karpenko, M. "A Review of Pseudospectral Optimal Control: From Theory to Flight," *Annual Reviews in Control*, Vol. 36, No. 2, pp. 182–197, 2012.

[16]Kalman, R. E., "Toward a Theory of Difficulty in Computation of Optimal Control," *Proceedings of the IBM Scientific Computing Symposium on Control Theory and Applications*, White Plains, N.Y. 1966. pp. 25-43.

[17]Ross, I. M., "A Roadmap for Optimal Control: The Right Way to Commute," *Annals of the New York Academy of Sciences*, Vol. 1065, No. 1, New York, N.Y., 2005, pp. 210-231.

[18]Boyd, J., *Chebyshev and Fourier Spectral Methods,* Dover Publications, Inc., Minola, New York, 2001.

[19]Gong, Q., Kang, W. and Ross, I. M., "A Pseudospectral Method for the Optimal Control of Constrained Feedback Linearizable Systems," *IEEE Transactions on Automatic Control*, Vol. 51, No. 7, July 2006, pp. 1115-1129.

[20]Gong, Q., Fahroo, F., and Ross, I. M. "A Spectral Algorithm for Pseudospectral Methods in Optimal Control", *Journal of Guidance, Control and Dynamics*, Vol. 31, No. 3, pp. 460–471, 2008.

[21]Elnagar, J., Kazemi, M. A. and Razzaghi, M., "The Pseudospectral Legendre Method for Discretizing Optimal Control Problems," *IEEE Transactions on Automatic Control,* Vol. 40, No. 10, 1995, pp. 1793-1796.

[22]Ross, I. M., and Fahroo, F., "Legendre Pseudospectral Approximations of Optimal Control Problems," *Lecture Notes in Control and Information Sciences*, Vol. 295, Springer-Verlag, New York, 2003.

[23]Elnagar, G., and Kazemi, M. A., "Pseudospectral Chebyshev Optimal Control of Constrained Nonlinear Dynamical Systems," *Computational Optimization and Applications*, Vol. 11, 1998, pp. 195-217.

[24]Fahroo, F. and Ross, I. M., "Direct Trajectory Optimization by a Chebyshev Pseudospectral Method," *Journal of Guidance, Control and Dynamics*, Vol. 25, No. 1, 2002, pp.160-166.

[25]Fahroo, F. and Ross, I. M. "Convergence of the Costates Does Not Imply Convergence of the Control," *Journal of Guidance, Control and Dynamics*, Vol. 31, No. 5, pp. 1492–1497, 2008.

[26]Fahroo, F. and Ross, I. M. "Advances in Pseudospectral Methods for Optimal Control," *AIAA Guidance, Navigation, and Control Conference,* AIAA Paper 2008-7309. 2008.

[27]Gong, Q., Ross, I. M., and Fahroo, F., "Pseudospectral Optimal Control on Arbitrary Grids," *Advances in the Astronautical Sciences*, Vol. 135, Astrodynamics 2009, Univelt, San Diego, CA. AAS 09-405.

[28]Kang, W., Ross, I. M., and Gong, Q., "Pseudospectral Optimal Control and its Convergence Theorems," *Analysis and Design of Nonlinear Control Systems*, Springer-Verlag, Berlin Heidelberg, 2008, pp. 109–126.

[29]Ross, I. M. *A Beginner's Guide to DIDO: A MATLAB Application Package for Solving Optimal Control Problems*, Elissar Global, Carmel, CA, November 2007. http://www.elissarglobal.com/industry/products/

[30]Bedrossian, N., Bhatt, S., Kang, W., and Ross, I. M., "Zero-Propellant Maneuver Guidance," *IEEE Control Systems Magazine*, October 2009, pp. 53–73.

[31]Gong, Q., Kang, W., Bedrossian, N., Fahroo, F., Sekhavat, P. and Bollino, K., *Pseudospectral Optimal Control for Military and Industrial Applications*, Special Session of the *46th IEEE Conference on Decision and Control*, New Orleans, LA, pp. 4128-4142, Dec. 2007.

[32]Bedrossian, N., Karpenko, M., and Bhatt, S., "Overclock My Satellite: Sophisticated Algorithms Boost Satellite Performance on the Cheap," *IEEE Spectrum*, November 2012.

[33]Kang, W. and Bedrossian, N., "Pseudospectral Optimal Control Theory Makes Debut Flight – Saves NASA $1M in Under 3 hrs," *SIAM News*, Vol. 40, No. 7, September 2007, Page 1.

[34]Beals, G. A., Crum, R. C., Dougherty, H. J., Hegel, D. K., Kelley, J. L., and Rodden, J. J., "Hubble Space Telescope Precision Pointing Control System," *Journal of Guidance, Control and Dynamics*, Vol. 11, No. 2, 1988, pp. 119-123.

[35]Thienel, J. K., and Sanner, R. M., "Hubble Space Telescope Angular Velocity Estimation During the Robotic Servicing Mission," *Journal of Guidance, Control, and Dynamics*, Vol. 30, No. 1, 2007, pp. 29-34.

[36]Karpenko, M., Bhatt, S., Bedrossian, N., Fleming, A., and Ross. I. M., "First Flight Results on Time-Optimal Spacecraft Slews," *Journal of Guidance Control and Dynamics*, Vol. 35, No. 2, 2012, pp. 367-376.

[37]Karpenko, M., and Ross, I. M., "Implementation of Shortest-Time Maneuvers for Generic CMG Steering Laws," *Proceedings of the AIAA/AAS Astrodynamics Specialist Conference*, August 13-16, 2012, Minneapolis, MN, Paper Number: AIAA 2012-4959.

[38]Karpenko, M., Bhatt, S., Bedrossian, N., and Ross, I. M., "Flight Implementation of Shortest-Time Maneuvers for Imaging Satellites," *Journal of Guidance, Control, and Dynamics*, to appear.

[39]Sidi, M.J., *Spacecraft Dynamics and Control,* Cambridge University Press, New York, NY, 1997.

[40]Julier, S. J., "The Spherical Simplex Unscented Transformation," *Proceedings of the American Control Conference*, Denver, CO, June 4-6, 2003, Vol. 3, Pages 2430-2434.